



Intelligent prediction of rock mass deformation modulus through three optimized cascaded forward neural network models

Mahdi Hasanipanah¹ · Mehdi Jamei² · Ahmed Salih Mohammed³ · Menad Nait Amar⁴ · Ouaer Hocine⁵ · Khaled Mohamed Khedher^{6,7}

Received: 12 March 2022 / Accepted: 18 May 2022 / Published online: 31 May 2022
© The Author(s), under exclusive licence to Springer-Verlag GmbH Germany, part of Springer Nature 2022

Abstract

Rock mass deformation modulus (E_m) is a key parameter that is needed to be determined when designing surface or underground rock engineering constructions. It is not easy to determine the deformability level of jointed rock mass at the laboratory; thus, researchers have suggested different in-situ test methods. Today, they are the best methods; though, they have their own problems: they are too costly and time-consuming. Addressing such difficulties, the present study offers three advanced and efficient machine-learning methods for the prediction of E_m . The proposed models were based on three optimized cascaded forward neural network (CFNN) using the Levenberg–Marquardt algorithm (LMA), Bayesian regularization (BR), and scaled conjugate gradient (SCG). The performance of the proposed models was evaluated through statistical criteria including coefficient of determination (R^2) and root mean square error (RMSE). The computational results showed that the developed CFNN-LMA model produced better results than other CFNN-SCG and CFNN-BR models in predicting the E_m . In this regard, the R^2 and RMSE values obtained from CFNN-LMA, CFNN-SCG, and CFNN-BR models were equal to (0.984 and 1.927), (0.945 and 2.717), and (0.904 and 3.635), respectively. In addition, a sensitivity analysis was performed through the relevancy factor and according to its results, the uniaxial compressive strength (UCS) was the most impacting parameters on E_m .

Keywords Rock mass deformation modulus · Cascaded forward neural network · Prediction models · Optimization

Communicated by: H. Babaia

✉ Mahdi Hasanipanah
Hasanipanahmahdi@duytan.edu.vn

¹ Institute of Research and Development, Duy Tan University, Da Nang 550000, Vietnam

² Faculty of Engineering, Shohadaye Hoveizeh Campus of Technology, Shahid Chamran University of Ahvaz, Dashte Azadegan, Iran

³ Civil Engineering Department, College of Engineering, University of Sulaimani, Kurdistan Region, Iraq

⁴ Département Études Thermodynamiques, Division Laboratoires, Sonatrach, Boumerdes, Algeria

⁵ Laboratoire Génie Physique Des Hydrocarbures, Faculté Des Hydrocarbures Et de La Chimie, Université M'Hamed Bougara de Boumerdes, Avenue de l'Indépendance, 35000 Boumerdes, Algeria

⁶ Department of Civil Engineering, College of Engineering, King Khalid University, Abha 61421, Saudi Arabia

⁷ Department of Civil Engineering, High Institute of Technological Studies, Mrezgua University Campus, Nabeul 8000, Tunisia

Introduction

To design and execute the rock engineering constructions successfully, it is of a high importance to predict the rock mass deformation modulus (E_m) since it best represents the pre-failure mechanical behaviors of rock mass (Gholamnejad et al. 2013; Fattahi 2016; Fattahi and Moradi 2018). Literature is consisted of a number of approaches proposed by different researchers to directly predict the E_m using in-situ tests; they include plate loading test (PLT), pressure meter (Chun et al. 2009), cable jack, plate jacking, radial jacking, flat jack, and add to the list the geophysical methods. Nowadays, such techniques are the best for this purpose; though they are costly and time-consuming, and only after the excavation operation, they can be done (Gholamnejad et al. 2013). Recently, an increasing number of empirical approaches have been proposed in literature for the prediction of the E_m . Bieniawski (1973) pioneered the empirical equations for this purpose; in his model, only rock mass rating (RMR) was considered as the input parameter. The

most important drawback of Bieniawski's approach was that it could be applied to rock masses with $RMR > 50$. On the other hand, attempting to remove this problem in the Bieniawski's equation, Serafim and Pereira (1983) introduced an equation for rock masses with $RMR < 50$. In addition, an empirical equation was introduced by Hoek and Brown (1997) on the basis of the geology strength index (GSI) and the uniaxial compressive strength (UCS) of intact rock. In two other studies, Nicholson and Bieniawski (1990) and Mitri et al. (1994) made the use of two modulus of the intact rock (E_i) in accordance with the value of RMR. Barton (2002) introduced a formula that included both UCS and tunneling quality index (Q) system. In another project, considering three parameters of rock quality designation (RQD), UCS, and weathering degree (WD) of rock, Gokceoglu et al. (2003) offered an empirical equation to literature. Kayabasi et al. (2003) discussed the relation on the basis of WD, E_i , and RQD. The empirical equation of Zhang and Einstein (2004) was based on E_i and RQD. On the other hand, the classification system of rock mass index (RMI) was a basis for Palmström and Singh (2001) to propose relations. In the Hoek and Diederichs's (2006) study, formulas were offered on the basis of GSI and D (factor of disturbance), while in Sonmez et al.'s (2004) research, they were on the basis of E_i , GSI, and D parameters.

In recent years, the use of computational intelligence methods have been highlighted in different engineering fields (Ray et al 2020; Hasanipanah and Amnieh 2020a, 2020b; Armaghani et al. 2020a, 2020b; Asteris et al. 2020, 2021a, b, 2022a, b; Zhou et al. 2021; Zhu et al. 2021; Du et al. 2022). For instance, Sonmez et al. (2006) utilized the artificial neural networks (ANNs) and Majdi and Beiki (2010) employed a hybrid system of ANNs and genetic algorithms (GA) for the prediction of E_m . On the other hand, an adaptive network-based fuzzy inference system (ANFIS) model was introduced by Gokceoglu et al. (2004) to effectively predict the E_m of jointed rock masses. Alemdag et al. (2016) predicted the E_m using ANN, ANFIS, and genetic programming (GP) models. According to their findings, the performance of GP was better than ANN and ANFIS models. A Monte Carlo simulation (MCS) was employed to predict E_m in the study conducted by Fattahi et al. (2019). They demonstrated that the MCS was an acceptable tool in this field. In another study, Majdi and Beiki (2019) used a fuzzy c-means clustering (FCM) method optimized by particle swarm optimization (PSO) and GA for the same purpose. Their results confirmed an acceptable performance of PSO and GA in optimizing the FCM model.

The present study investigates the use of three optimized cascaded forward neural network (CFNN) for predicting the E_m . For this work, the

Levenberg–Marquardt algorithm (LMA), Bayesian regularization (BR), and scaled conjugate gradient (SCG) procedures are used to optimize CFNN model. In other words, these algorithms were used in the training phase which consisted in the optimization of the weights and bias terms of CFNN. The rest of this paper is organized as follows. Material and Methods are provided in the next section. In the Material section, more explanations about the database is mentioned. Also, in the Methods section, the predictive models are explained. Then, in the next sections, we discussed the performance of the developed models in predicting the E_m , and finally the conclusions are stated.

Material and methods

Material

To develop the models proposed in this study, the requirement datasets were borrowed from Chun et al. (2009). In this database, sixty sets of data were prepared using several independent parameters and one dependent parameter (E_m).

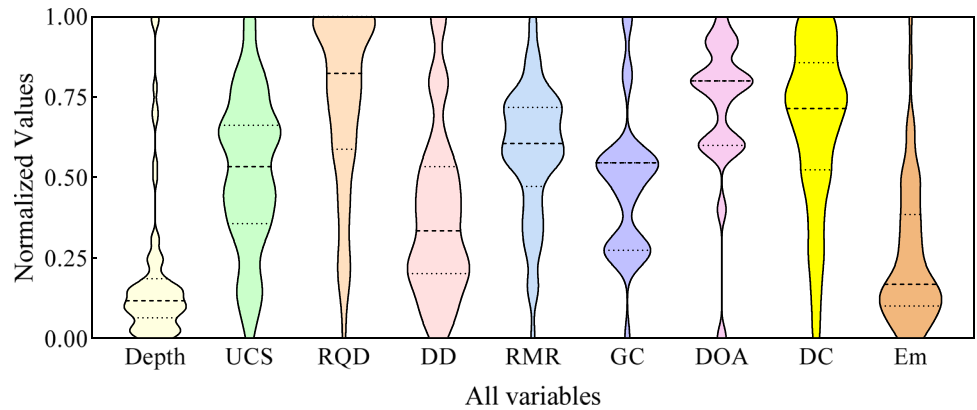
Data pre-processing one of the most important steps before providing computational intelligence methods which is significantly vital in selecting the properly data-driven model for yielding the favourable accuracy. In this research, eight variables including depth of the measurement of E_m , UCS, RQD, discontinuity density (DD), RMR, ground water Condition (GC), discontinuity orientation adjustment (DOA), and discontinuity condition (DC) were used as inputs and E_m was used as the output. Table 1 listed the descriptive statistics of all variables. The statistical properties of all the inputs show that the diversity of datasets except depth and DOA parameters are at a suitable level. Of all the input variables, UCS and RMR are the closest to the normal distribution due to having the smallest distance between the mean and median. Figure 1 demonstrates the normalized values probability distribution of all datasets. According to Fig. 1 and results of Table 1, the depth and DOA have the highest skewness (2.333 and -1.664, respectively) and kurtosis (5.127 and 3.481, respectively) among all datasets and consequently both of them deviate more from the normal distribution than the other variables. The statistical analysis of used datasets acknowledges the need for a robust AI model for modelling the E_m .

Figure 2 demonstrates the correlogram of all utilized variables. Clearly, it can be seen that the DD, UCS, and RMS

Table 1 Secretive statistics of implemented datasets for the E_m prediction

Statistics	Inputs								Output
	Depth	UCS	RQD	DD	RMR	GC	DOA	DC	E_m
Minimum	4.000	12.100	3.000	5.000	21.000	4.000	-25.000	9.000	3.920
Q25%	14.250	98.500	13.000	8.000	54.500	7.000	-10.000	20.000	8.085
Median	22.800	141.600	17.000	10.000	64.000	10.000	-5.000	24.000	10.890
Q75%	33.850	172.800	20.000	13.000	72.000	10.000	-5.000	27.000	19.960
Maximum	166.000	254.800	20.000	20.000	92.000	15.000	0.000	30.000	45.620
Mean	33.870	138.100	15.520	10.840	62.230	9.267	-7.133	22.880	14.590
Std. Dev	36.620	58.610	4.660	3.990	14.590	2.449	5.543	5.396	9.114
Skewness	2.333	-0.156	-0.953	0.803	-0.636	0.547	-1.664	-0.766	1.301
Kurtosis	5.127	-0.547	-0.027	-0.030	0.410	0.572	3.481	-0.032	1.581

Fig. 1 Distribution of normalized values of all implemented variables in the modelling



variables due to having the highest Pearson correlation coefficients (0.727, 0.716, and 0.694, respectively) are identified as the most influential parameters and GC by lowest Pearson correlation coefficient (0.035) has the least impact on the E_m modelling.

Methods

Cascaded forward neural network (CFNN)

Further rigorous paradigms of ANN called CFNN is largely used as it ensures reliable results when modelling highly complicated systems. The topology of the aforementioned model belongs to the feedforward kind, which is based highly on back-propagation (BP) strategy to refurbish the weights during the learning process (Nait Amar 2020). Three kinds of layers can be considered in a CFNN paradigm, i.e., input, output, and hidden layers. The feature of this model is that the hidden layers are developed in a cascade structure by generating more neurons and interactions along with the whole of inputs and previous hidden neurons (Nait Amar 2020). The CFNN cascade form lets every neuron of the prior layer to be relied upon with the neurons of the next layers (Abujazar et al. 2018). The preferable number of hidden layers, their numbers of neurons and their activation functions in a CFNN model are frequently examined using trial and error method.

The learning phase of CFNN model focuses to achieve suitable values of weights and bias that lead to minimize the quadratic error outlining the gap between the predictions and the true values. To this end, back-propagation (BP)

Correlogram of variables

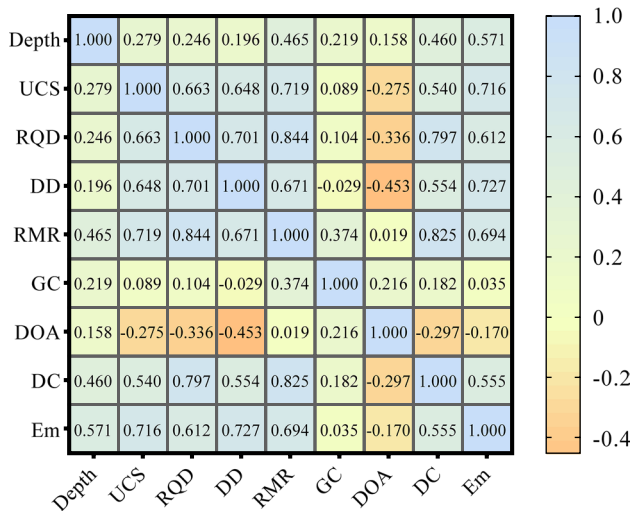


Fig. 2 Correlogram of all variables used in E_m prediction

algorithms are the most widespread used thanks to their excellent results provided. In this paper, three alternative approaches namely, Levenberg–Marquardt (LM) algorithm, Bayesian regularization (BR), and scaled conjugate gradient (SCG) are applied, and which will be explained in the next section.

Optimization techniques

Levenberg–Marquardt algorithm (LMA)

The LMA represents one of the most advantageous optimization techniques which are applied to find solutions to the nonlinear least square issues. The stated method has the ability to locate the ultimate solution even from an unsuitable initial hypothesis, but it does not conduct to global minimization. For this technique, the optimization procedure refers to that of Newton's method, but they differ fairly in their conceptions. In LMA, the Hessian matrix is approximated, in addition to the introduction of a regularization parameter that ameliorates the calculation procedure. The approximations of the Hessian matrix and the gradient are shown in the formulas below (Kişi and Uncuoglu 2005):

$$H = J^T J \quad (1)$$

$$g = J^T e \quad (2)$$

with J and e denote the Jacobian matrix and the error vector, respectively, whereas T stands for the transposition operator. The LMA step can be updated as mentioned in Eq. (3) by replacing the approximated Hessian and gradient matrixes and by inserting the regularization parameter in the fundamental formula of Newton's technique:

$$x_{i+1} = x_i - (H - \eta I)^{-1} \times g \quad (3)$$

where i and η represent the iteration and the regularization parameter, respectively, otherwise, x denotes the weights.

Bayesian regularization (BR)

The optimization of weights and bias using Bayesian regularization (BR) technique is inspired from LMA approach (MacKay 1992; Foresee and Hagan 1997). Indeed, the concept of BR algorithm is to minimize an objective function, which involves a weighted summation of squared error and squared network weights (Yue et al. 2011). The network weights for the objective function in BR is determined as shown below:

$$F(w) = \alpha E_w + \beta E_D \quad (4)$$

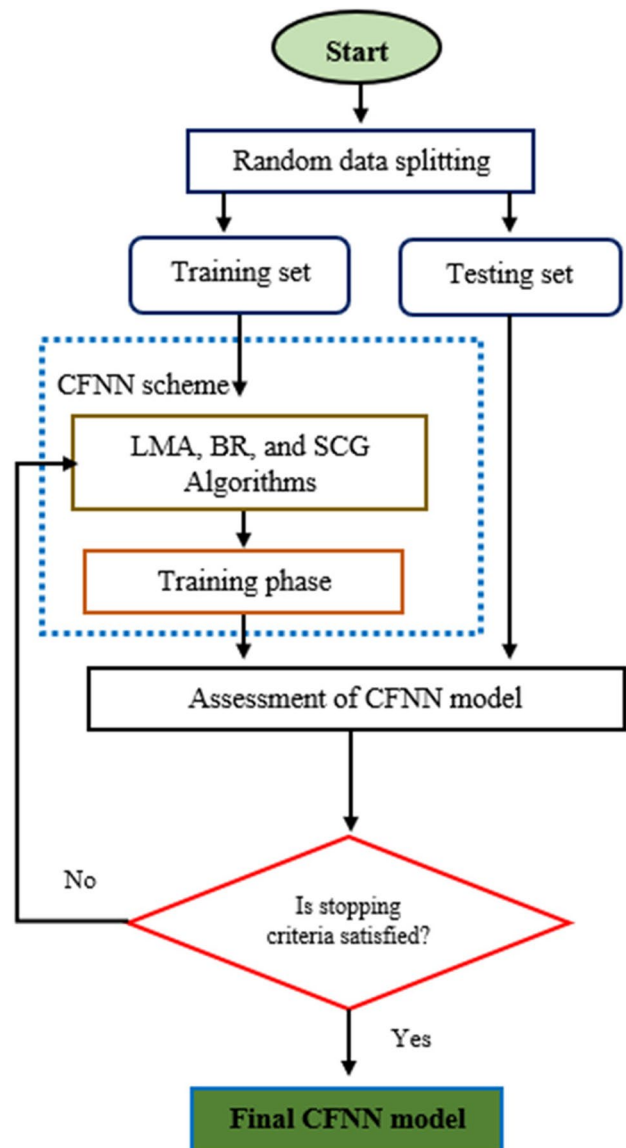
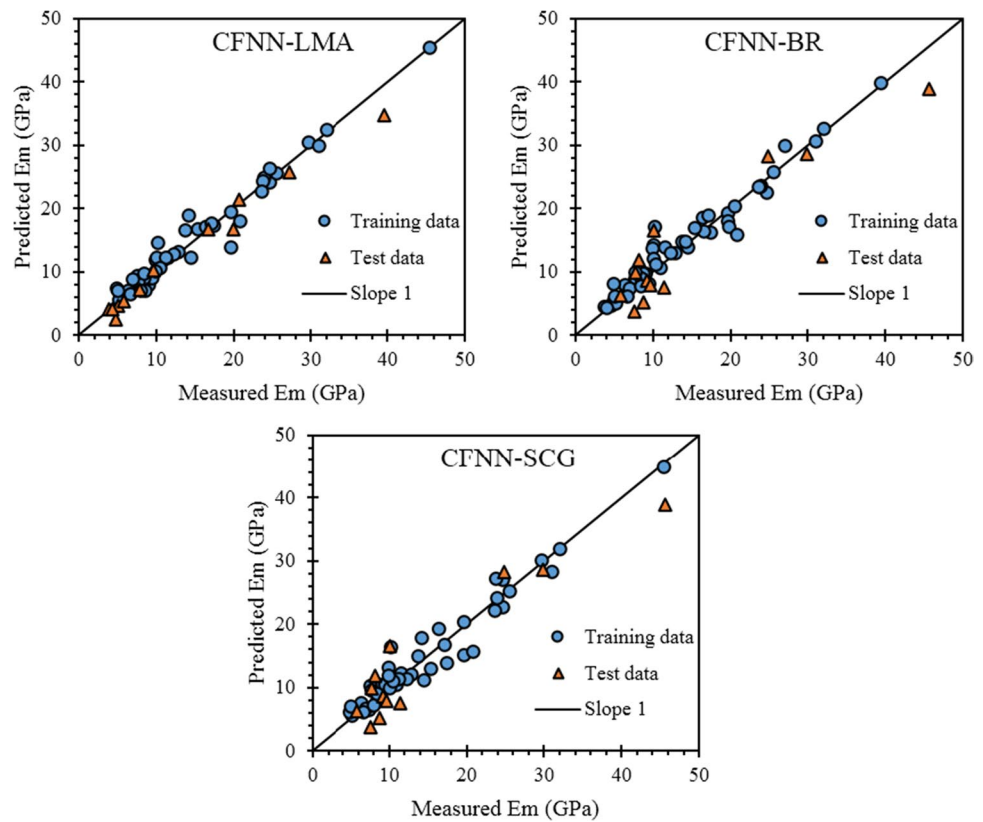


Fig. 3 Workflow of the implementation procedure

In the above-equation, E_w and E_D indicate the sum of squared network weights and the sum of network errors, correspondingly, however α and β denote the objective function $F(w)$ parameters. The two aforementioned parameters are provided from the theorem of Bayes. To this end, a Gaussian type distribution is relied to choose the training set and determine the weight vector. The training sets selection with some manipulation of algebraic operations lead to the optimum values of α and β . After that, a minimization of $F(w)$ and an updating of weights is realized by using the LM algorithm. This calculation steps are repeated until reaching a stopping criterion (Yue et al. 2011).

Fig. 4 Cross plots of the suggested CFNN models



Scaled conjugate gradient (SCG)

One of most discussed issues of the conventional back-propagation technique that uses the negative descent direction approach to update the weights is the shortage of convergence speed (Yue and Songzheng 2011). The conjugate gradient represents an alternative strategy to remedy this issue, and the error minimization acquired previously is kept as follows:

$$P_0 = -g_0 \tag{5}$$

with P_0 represents the conjugate direction and $-g_0$ means the search direction. In this algorithm, the purpose of the best distance determination is for optimizing the actual search direction. The following equation leads to calculate the proper distance (Kişi and Uncuoglu 2005):

$$x_{i+1} = x_i + \alpha_i g_i \tag{6}$$

Then, the search direction is determined using the next formula (Kişi and Uncuoglu 2005):

$$P_0 = -g_0 + \beta_i P_{i-1} \tag{7}$$

A variety of conjugate algorithm versions can be apprehended according to the β determination steps (Kişi and Uncuoglu 2005). It should be noted that the line search is a computational method but it is expensive, thus, it is preferable to use other cheaper techniques such as the scaled conjugate gradient

(SCG). The latter technique incorporates the CG algorithm with trust region technique (Møller 1993).

Development procedure

The database compiled from the published literature was divided into training and testing sets for utilizations in the training and test phases of CFNN model, respectively. The training set involved 80% of the collected measurements, while 20% of the points were devoted for the test set. It is worth mentioning that the different variables of this amassed database were normalized between -1 and 1 using the following formula:

$$Var_n = \frac{2(Var_i - Var_{min})}{(Var_{max} - Var_{min})} - 1 \tag{8}$$

where Var_{max} and Var_{min} represent the maximum and minimum values of a specified variable, respectively, and Var_n points out its normalized value.

The prediction reliability of CFNN model depends greatly on the appropriate selection of its control parameters, such as its topology, the activation functions of the hidden layers, as well as the techniques applied for optimizing the weights and bias terms of the network. To this end, the trial and error technique was applied for investigating the suitable numbers of hidden layers, their number of neurons, and their

activation functions. Besides, and as mentioned in the previous section, three rigorous back-propagation based techniques, including LMA, BR, and SCG were implemented for optimizing the weights and bias of the CFNN model. The gained models were denoted CFNN-LMA, CFNN-BR, and CFNN-SCG, respectively. The workflow of Fig. 3 summarizes the steps of the implementation using these aforesaid algorithms.

Results and discussion

After carrying out the described implementation steps, it was found that the three paradigms, i.e., CFNN-LMA, CFNN-BR, and CFNN-SCG involved two hidden layers with 12 and 9 neurons in each of them, respectively. The most suitable activation function in the hidden layers of these CFNN models was *Tansig*.

The models were evaluated statistically and graphically using various criteria. The graphical evaluation was carried out through cross plot for examining the integrity of the developed paradigms and histogram of error distribution, which aimed at detecting any likely error trend. Coefficient of determination (R^2) and Root mean square error (RMSE) were the main statistical indexes that were used in the assessment of the prediction performance of the gained models. These indexes are expressed as follows (Hasanipanah et al. 2015; Nikafshan Rad et al. 2019; Hasanipanah et al. 2020a, b, c; Armaghani and Asteris 2021; Parsajoo et al. 2021; Li et al. 2021; Ly et al. 2021; Karir et al. 2022):

1. Coefficient of Determination (R^2).

$$R^2 = 1 - \frac{\sum_{j=1}^N (Em_{j_{exp}} - Em_{j_{pred}})^2}{\sum_{j=1}^N (Em_{j_{pred}} - \overline{Em})^2} \quad (9)$$

2. Root Mean Square Error (RMSE).

$$RMSE = \sqrt{\frac{1}{N} \sum_{j=1}^N (Em_{j_{exp}} - Em_{j_{pred}})^2} \quad (10)$$

In the above-equations, the subscripts *exp* and *pred* denote the real and estimated values of E_m , respectively, \overline{Em} is the average value of E_m , and N represents the number of samples.

Cross plots of observed E_m values and those predicted by the implemented CFNN paradigms are exhibited in Fig. 4. For a given model, it can be said that it generates good prediction performance if a light cloud of its predictions is noticed near the line $X = Y$ (unit-slope

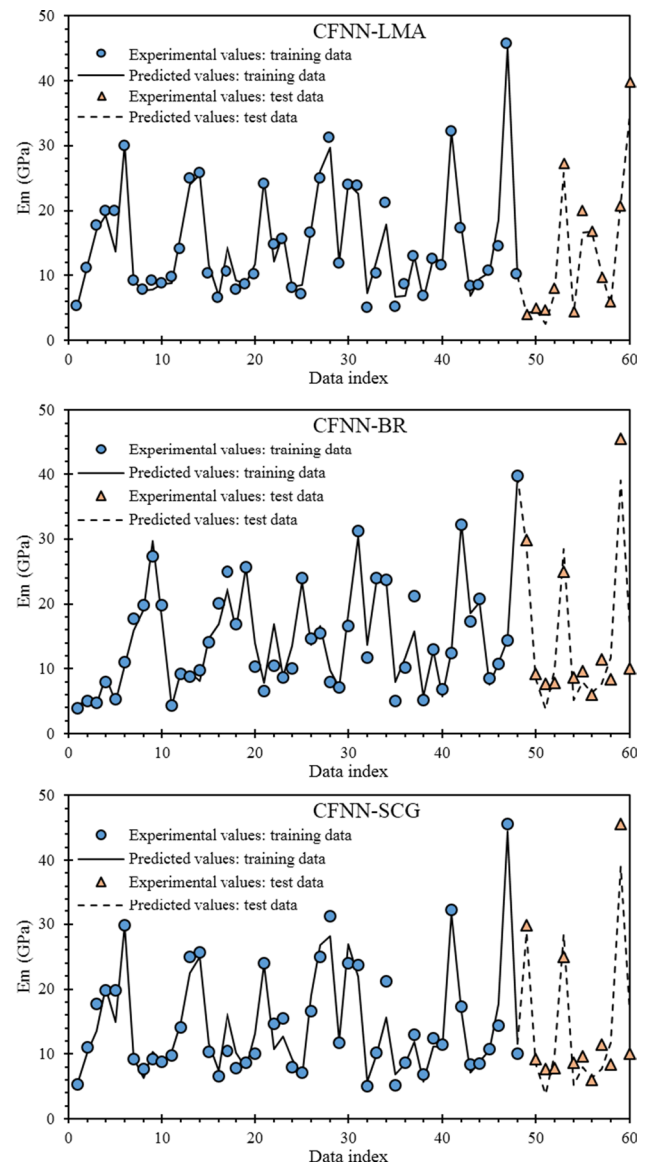


Fig. 5 Comparison between the observed E_m values and the predictions of the suggested CFNN models versus data index during the training and test phases

line). As shown in the cross plots of Fig. 4, the predictions of the suggested paradigms are well-distributed around the reference line $X = Y$ for both training testing phases. Deviations of the E_m values estimated by the newly proposed models from the real data during the training and testing phases are also illustrated in subplots a-c of Fig. 5, for CFNN-LMA, CFNN-BR, and CFNN-SCG, respectively. According to this figure, a satisfactory agreement exists between E_m predicted by CFNN-LMA, CFNN-BR, and CFNN-SCG and the real values of the database.

In another kind of evaluation, the distributions of the noticed errors between the estimations of the three

Fig. 6 Histogram diagrams of the errors associated with the predictions of the suggested CFNN models

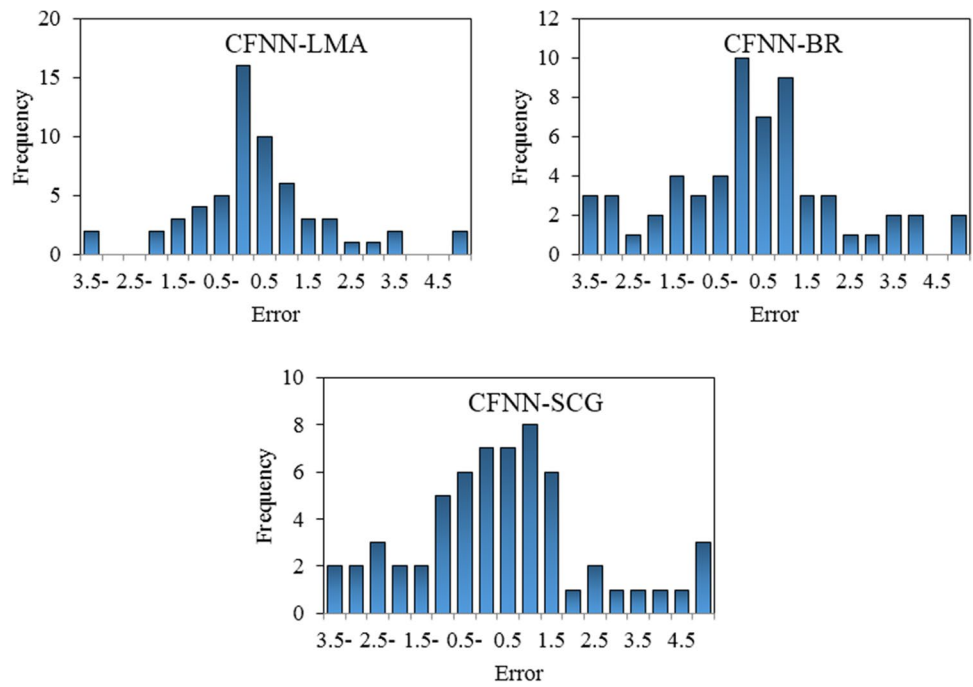


Table 2 Statistical evaluation of the suggested CFNN models

Sorting of data	Statistical indexes	CFNN-LMA	CFNN-BR	CFNN-SCG
Training data	RMSE	1.6605	1.8276	2.0985
	R^2	0.9623	0.9516	0.9399
Test data	RMSE	1.927	3.6358	2.7175
	R^2	0.9842	0.9042	0.9448

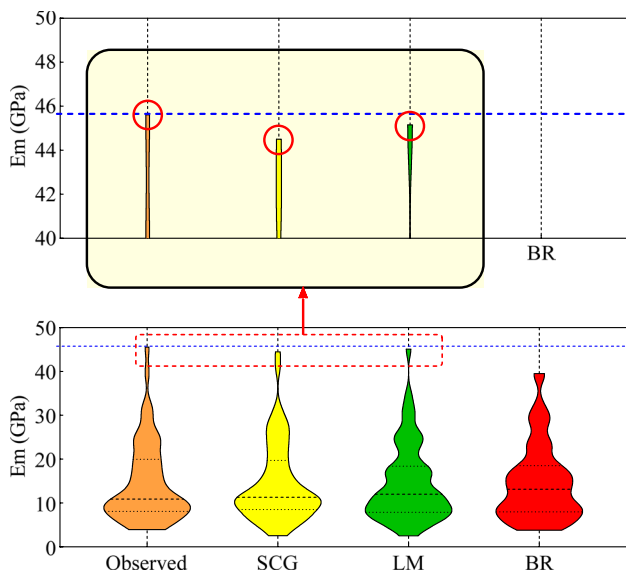


Fig. 7 The probability density function of observed and predicted E_m values

paradigms and actual data are demonstrated in histogram diagrams of Fig. 6. As can be seen, a normal distribution of the associated errors with a centre equal to or very close to zero-error value is achieved in all of the models. This kind of distribution indicates the high reliability of the newly proposed CFNN models.

For a detailed assessment of the global integrity of the suggested paradigms, Table 2 states the statistical indexes, namely R^2 and RMSE, of these models for training, test, and overall data sets. As indicated in this table, the reliability of CFNN models is clearly deemed for the different data sets as these paradigms achieved high R^2 and small RMSE values for these sets. By taking a deeper look to the performance evaluation reported in Table 2 and Figs. 4, 5 and 6, it can be said that although the good prediction performance of the proposed models, CFNN-LMA showed a higher ability and a more reliability compared with CFNN-BR and CFNN-SCG when estimating E_m values of the different cases included in the database.

Fig. 8 The cumulative frequency of relative deviation (%) for three models

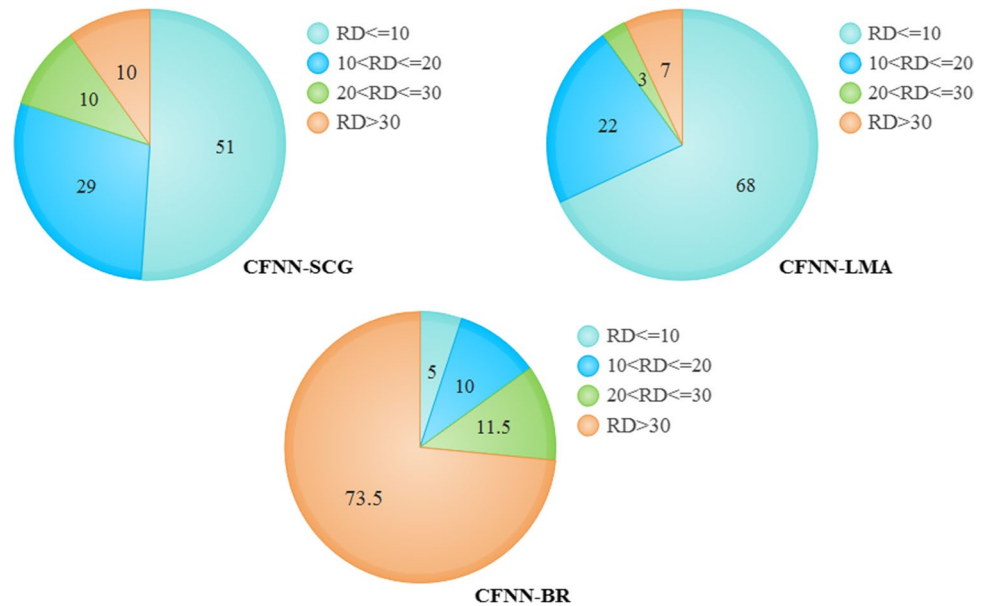


Fig. 9 Evaluation of the importance of the input parameters on E_m using the relevancy factor

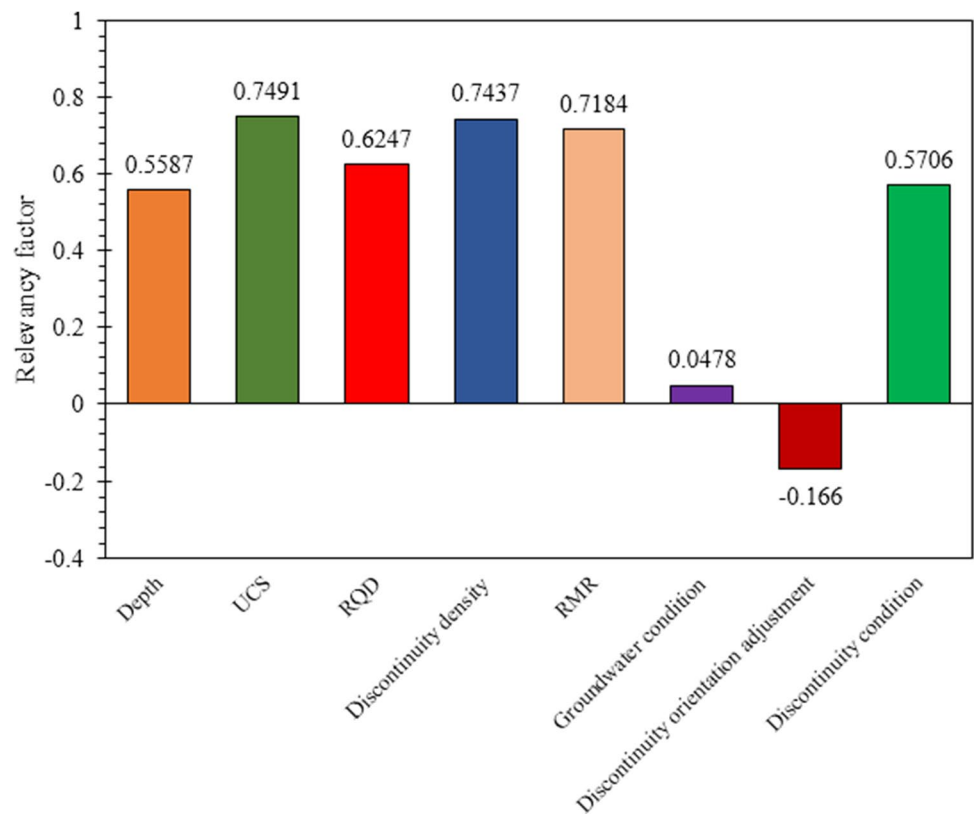


Figure 7 illustrates the probability distribution function (PDF) of observed and predicted E_m values for better models validation. This Fig demonstrated the PDFs with corresponding each optimized CFNN models for all data sets (training and testing stages). The comparing the PDF of each model demonstrated that the CFNN-LMA yielded

better agreement with the observed datasets. Besides, the quartiles values ($Q_{25\%}$, median, and $Q_{75\%}$) of three provided models showed that the CFNN-LMA on account of closest quartile ($Q_{25\%} = 7.908$ and $Q_{75\%} = 19.75$) is more consistent with the observational datasets ($Q_{25\%} = 8.085$ and $Q_{75\%} = 19.96$) in comparison with CFNN-CG ($Q_{25\%} = 8.538$

and $Q_{75\%} = 19.35$) and CFNN-BR ($Q_{25\%} = 7.96$ and $Q_{75\%} = 18.53$) models. Thus, I can be conclude that the CFNN-LMA yields more promising results than other two models for prediction of E_m values.

In the last error validation of model, the cumulative frequency of relative deviation (CFRD) values for three models were examined and depicted in Fig. 8. The results indicated that in the CFNN-LMA, more than 68% of whole datasets have ($RD \leq 10\%$) and only 7% of all data sets yielded to ($RD > 30\%$) whereas in CFNN-SCG model, 51% and 10% of all data sets led to ($RD \leq 10\%$) and, ($RD > 30\%$) respectively. Besides, the CFNN-BR model is introduced as the worst performance among three presented methods because it caused 70% of the data sets to lead to more than 30% relative deviation.

In the last step of this work, a sensitivity analysis was carried out on our best paradigm, i.e., CFNN-LMA, to determine the impact of each of the included variables on E_m . To gain this, the relevancy factor (r) (Shateri et al. 2015; Nait Amar and Jahanbani Ghahfarokhi 2020; Nait Amar et al. 2021) was computed. It is worth mentioning that the value of this factor demonstrates the impact degree of a given variable, while its sign exhibits the positive or the negative effect of a variable on the output. The relevancy factor is calculated using the following formula:

$$r(Inp_j, O) = \frac{\sum_{i=1}^N (Inp_{j,i} - \overline{Inp_j})(O_i - \overline{O})}{\sqrt{\sum_{i=1}^N (Inp_{j,i} - \overline{Inp_j})^2 \sum_{i=1}^N (O_i - \overline{O})^2}} \tag{11}$$

In the above-equation, the data index is specified by the subscript i ; I_j and $\overline{I_j}$ point out the j^{th} variable and its average value, respectively, and O and \overline{O} refer to the estimated value of the output and its average, respectively.

Figure 9 displays the evaluation of the impact of the variables using the relevancy factor. As can be seen, only discontinuity orientation adjustment has a negative effect on E_m values, while the other input parameters have positive impact on E_m . From the degree of importance perspective, UCS and discontinuity density are the most impacting parameters on E_m with r values of 0.7491 and 0.7437, respectively, while groundwater condition has the weakest effect on E_m with an r value of 0.0478.

Conclusions

The main purpose of this study is to develop three optimized models, i.e. CFNN-LMA, CFNN-BR and CFNN-SCG to predict E_m . When designing surface or underground rock engineering constructions, the prediction of E_m is a

significant subject, and using the advanced machine learning methods can be useful in this field. Therefore, the authors of this study have tried to propose efficient models to accurately predict E_m . To develop the proposed models, we adopted the datasets formerly presented by Chun et al. (2009). Totally, eight effective parameters on E_m were used as the input parameters by using sixty sets of data. Then, R^2 and RMSE, as two common error indexes, were computed to check the accuracy of the developed models. The following findings can be drawn from the analysis and results:

- According to the obtained results, the CFNN-LMA model predicted the E_m with the RMSE of 1.927 and R^2 of 0.984. These values for CFNN-SCG models were 0.945 and 2.717, and also for CFNN-BR model were 0.904 and 3.635. Therefore, the lowest RMSE and the highest R^2 were obtained from CFNN-LMA model. This indicates the superiority of the CFNN-LMA model in comparison with CFNN-BR and CFNN-SCG models for predicting E_m .
- Comparing the probability distribution function (PDF) of each developed model showed that the CFNN-LMA yielded better agreement with the observed datasets. Furthermore, based on the cumulative frequency of relative deviation (CFRD), the best results were obtained from CFNN-LMA model. The above results confirm the effectiveness of CFNN-LMA model in this field.
- In this study, a sensitivity analysis was also performed through the relevancy factor and according to the calculations, only discontinuity orientation adjustment had a negative effect on E_m values, and other input parameters had positive impact on E_m . Also, it was found that the UCS and discontinuity density were the most impacting parameters on E_m .

Declarations

Conflict of interest The authors declare that they have no competing interests.

References

Abujazar MSS, Fatihah S, Ibrahim IA, Kabeel AE, Sharil S (2018) Productivity modelling of a developed inclined stepped solar still system based on actual performance and using a cascaded forward neural network model. *J Clean Prod* 170:147–159

Alemdag S, Gurocak Z, Cevik A, Cabalar AF, Gokceoglu C (2016) Modeling deformation modulus of a stratified sedimentary rock mass using neural network, fuzzy inference and genetic

- programming. *Eng Geol* 203:70–82. <https://doi.org/10.1016/j.enggeo.2015.12.002>
- Armaghani DJ, Asteris PG (2021) A comparative study of ANN and ANFIS models for the prediction of cement-based mortar materials compressive strength. *Neural Comput Appl* 33(9):4501–4532
- Armaghani DJ, Asteris PG, Fatemi SA et al (2020) On the use of neuro-swarm system to forecast the pile settlement. *Appl Sci* 10:1904
- Armaghani DJ, Mirzaei F, Toghrol A, Shariati A (2020) Indirect measure of shear strength parameters of fiber-reinforced sandy soil using laboratory tests and intelligent systems. *Geomech Eng* 22(5):397–414. <https://doi.org/10.12989/gae.2020.22.5.397>
- Asteris PG, Apostolopoulou M, Armaghani DJ et al (2020) On the metaheuristic models for the prediction of cement-metakaolin mortars compressive strength. *Metaheuristic Comput Appl* 1(1):63–99. <https://doi.org/10.12989/mca.2020.1.1.063>
- Asteris PG, Lemonis ME, Le TT, Tsavdaridis KD (2021) Evaluation of the ultimate eccentric load of rectangular CFSTs using advanced neural network modeling. *Eng Struct* 248. <https://doi.org/10.1016/j.engstruct.2021.113297>
- Asteris PG, Skentou AD, Bardhan A, Samui P, Lourenço PB (2021) Soft computing techniques for the prediction of concrete compressive strength using Non-Destructive tests. *Constr Build Mater* 303
- Asteris PG, Gavriilaki E, Touloumenidou T et al (2022) Genetic prediction of ICU hospitalization and mortality in COVID-19 patients using artificial neural networks. *J Cell Mol Med*. <https://doi.org/10.1111/jcmm.17098>
- Asteris PG, Lourenço PB, Roussis PC et al (2022) Revealing the nature of metakaolin-based concrete materials using artificial intelligence techniques. *Constr Build Mater* 322
- Barton N (2002) Some new Q value correlations to assist in site characterization and tunnel design. *Int J Rock Mech Min Sci* 39:185–216. [https://doi.org/10.1016/S1365-1609\(02\)00011-4](https://doi.org/10.1016/S1365-1609(02)00011-4)
- Bieniawski Z (1973) Engineering classification of rock masses. *Trans S Afr Inst Civ Eng* 15:335–344
- Chun BS, Ryu WR, Sagong M, Do JN (2009) Indirect estimation of the rock deformation modulus based on polynomial and multiple regression analyses of the RMR system. *Int J Rock Mech Min Sci* 46:649–658. <https://doi.org/10.1016/j.ijrmmms.2008.10.001>
- Du K, Liu M, Zhou J, Khandelwal M (2022) Investigating the slurry fluidity and strength characteristics of cemented backfill and strength prediction models by developing hybrid GA-SVR and PSO-SVR. *Mining, Metallurgy & Exploration* 39(2):433–452
- Fattahi H (2016) Application of improved support vector regression model for prediction of deformation modulus of a rock mass. *Eng Comput* 32:567–580. <https://doi.org/10.1007/s00366-016-0433-6>
- Fattahi H, Moradi A (2018) A new approach for estimation of the rock mass deformation modulus: a rock engineering systems-based model. *Bull Eng Geol Environ* 77:363–374
- Fattahi H, Varmazyari Z, Babanouri N (2019) Feasibility of Monte Carlo simulation for predicting deformation modulus of rock mass. *Tunn Undergr Sp Technol* 89:151–156
- Foresee FD, Hagan MT (1997) Gauss–Newton approximation to Bayesian learning. In: *Proceedings of the international joint conference on neural networks*. Houston, TX, USA, June
- Gholamnejad J, Bahaaddini H, Rastegar M (2013) Prediction of the deformation modulus of rock masses using artificial neural networks and regression methods. *J Min Environ* 4:35–43. <https://doi.org/10.22044/jme.2013.144>
- Gokceoglu C, Sonmez H, Kayabasi A (2003) Predicting the deformation moduli of rock masses. *Int J Rock Mech Min Sci* 40:701–710. [https://doi.org/10.1016/S1365-1609\(03\)00062-5](https://doi.org/10.1016/S1365-1609(03)00062-5)
- Gokceoglu C, Yesilnacar E, Sonmez H, Kayabasi A (2004) A neuro-fuzzy model for modulus of deformation of jointed rock masses. *Comput Geotech* 31:375–383
- Hasanipanah M, Amnieh HB (2020) A fuzzy rule-based approach to address uncertainty in risk assessment and prediction of blast-induced flyrock in a quarry. *Nat Resour Res*. <https://doi.org/10.1007/s11053-020-09616-4>
- Hasanipanah M, Amnieh HB (2020) Developing a new uncertain rule-based fuzzy approach for evaluating the blast-induced backbreak. *Eng Comput*. <https://doi.org/10.1007/s00366-019-00919-6>
- Hasanipanah M, Monjezi M, Shahnazar A, Armaghani DJ, Farzmand A (2015) Feasibility of indirect determination of blast induced ground vibration based on support vector machine. *Measurement* 75:289–297
- Hasanipanah M, Keshtegar B, Thai DK et al (2020) An ANN adaptive dynamical harmony search algorithm to approximate the flyrock resulting from blasting. *Eng Comput*. <https://doi.org/10.1007/s00366-020-01105-9>
- Hasanipanah M, Meng D, Keshtegar B, Trung NT, Thai DK (2020) Nonlinear models based on enhanced Kriging interpolation for prediction of rock joint shear strength. *Neural Comput Appl*. <https://doi.org/10.1007/s00521-020-05252-4>
- Hasanipanah M, Zhang W, Armaghani DJ, Rad HN (2020) The potential application of a new intelligent based approach in predicting the tensile strength of rock. *IEEE Access* 8:57148–57157
- Hoek E, Brown E (1997) Practical estimates of rock mass strength. *Int J Rock Mech Min Sci* 34:1165–1186. [https://doi.org/10.1016/S1365-1609\(97\)80069-X](https://doi.org/10.1016/S1365-1609(97)80069-X)
- Hoek E, Diederichs M (2006) Empirical estimation of rock mass modulus. *Int J Rock Mech Min Sci* 43:203–215. <https://doi.org/10.1016/j.ijrmmms.2005.06.005>
- Karir D, Ray A, Bharati AK, Chaturvedi U, Rai R, Khandelwal M (2022) Stability prediction of a natural and man-made slope using various machine learning algorithms. *Transp Geotechn* 100745
- Kayabasi A, Gokceoglu C, Ercanoglu M (2003) Estimating the deformation modulus of rock masses: a comparative study. *Int J Rock Mech Min Sci* 40:55–63. [https://doi.org/10.1016/S1365-1609\(02\)00112-0](https://doi.org/10.1016/S1365-1609(02)00112-0)
- Kişçi Ö, Uncuoğlu E (2005) Comparison of three back-propagation training algorithms for two case studies. *Indian J Eng Mater Sci* 12(5):434–42. <http://nopr.niscair.res.in/handle/123456789/8460>
- Li E, Yang F, Ren M, Zhang X, Zhou J, Khandelwal M (2021) Prediction of blasting mean fragment size using support vector regression combined with five optimization algorithms. *J Rock Mech Geotech Eng* 13(6):1380–1397
- Ly HB, Pham BT, Le LM et al (2021) Estimation of axial load-carrying capacity of concrete-filled steel tubes using surrogate models. *Neural Comput Appl* 33(8):3437–3458
- MacKay DJ (1992) Bayesian interpolation. *Neural Comput* 4(3):415–447. <https://doi.org/10.1162/neco.1992.4.3.415>
- Majdi A, Beiki M (2010) Evolving neural network using a genetic algorithm for predicting the deformation modulus of rock masses. *Int J Rock Mech Min Sci* 47:246–253. <https://doi.org/10.1016/j.ijrmmms.2009.09.011>
- Majdi A, Beiki M (2019) Applying evolutionary optimization algorithms for improving fuzzy C-mean clustering performance to predict the deformation modulus of rock mass. *Int J Rock Mech Min Sci* 113:172–182. <https://doi.org/10.1016/j.ijrmmms.2018.10.030>
- Mitri HS, Edrissi R, Henning J (1994) Finite element modeling of cable bolted slopes in hard rock ground mines. In: *Proceedings of the SME annual meeting*, Albuquerque, New Mexico, February.

- Møller MF (1993) A scaled conjugate gradient algorithm for fast-supervised learning. *Neural Netw* 6:525–533. [https://doi.org/10.1016/S0893-6080\(05\)80056-5](https://doi.org/10.1016/S0893-6080(05)80056-5)
- Nait Amar M (2020) Modeling solubility of sulfur in pure hydrogen sulfide and sour gas mixtures using rigorous machine learning methods. *Int J Hydro Energy* 45:33274–33287
- Nait Amar M, Jahanbani Ghahfarokhi A (2020) Prediction of CO₂ diffusivity in brine using white-box machine learning. *J Pet Sci Eng* 190. <https://doi.org/10.1016/j.petrol.2020.107037>
- Nait Amar M, Ghriga MA, Ouaer H (2021) On the evaluation of solubility of hydrogen sulfide in ionic liquids using advanced committee machine intelligent systems. *J Taiwan Inst Chem Eng*. <https://doi.org/10.1016/j.jtice.2021.01.007>
- Nicholson G, Bieniawski Z (1990) A nonlinear deformation modulus based on rock mass classification. *Int J Min Geol Eng* 8:181–202. <https://doi.org/10.1007/BF01554041>
- Nikafshan Rad H, Hasanipanah M, Rezaei M, Eghlim AL (2019) Developing a least squares support vector machine for estimating the blast-induced flyrock. *Eng Comput* 34(4):709–717
- Palmström A, Singh R (2001) The deformation modulus of rock masses—comparisons between in situ tests and indirect estimates. *Tunn Undergr Sp Technol* 16:115–131. [https://doi.org/10.1016/S0886-7798\(01\)00038-4](https://doi.org/10.1016/S0886-7798(01)00038-4)
- Parsajoo M, Armaghani DJ, Asteris PG (2021) A precise neuro-fuzzy model enhanced by artificial bee colony techniques for assessment of rock brittleness index. *Neural Comput Appl*. <https://doi.org/10.1007/s00521-021-06600-8>
- Ray A, Kumar V, Kumar A et al (2020) Stability prediction of Himalayan residual soil slope using artificial neural network. *Nat Hazards* 103(3):3523–3540
- Serafim JL, Pereira JP (1983) Considerations on the Geomechanical Classification of Bieniawski. *Proceedings of International Symposium on Engineering Geology and Underground Openings, Lisbon*, pp 1133–1144
- Shateri M, Ghorbani S, Hemmati-Sarapardeh A, Mohammadi AH (2015) Application of Wilcoxon generalized radial basis function network for prediction of natural gas compressibility factor. *J Taiwan Inst Chem Eng* 50:131–141. <https://doi.org/10.1016/j.jtice.2014.12.011>
- Sonmez H, Ulusay R, Gokceoglu C (2004) Indirect determination of the modulus of deformation of rock masses based on the GSI system. *Int J Rock Mech Min Sci* 41:849–857. <https://doi.org/10.1016/j.ijrmmms.2003.01.006>
- Sonmez H, Gokceoglu C, Nefeslioglu H, Kayabasi A (2006) Estimation of rock modulus: for intact rocks with an artificial neural network and for rock masses with a new empirical equation. *Int J Rock Mech Min Sci* 43:224–235. <https://doi.org/10.1016/j.ijrmmms.2005.06.007>
- Yue Z, Songzheng Z, Tianshi L (2011) Bayesian regularization BP Neural Network model for predicting oil-gas drilling cost, BMEI 2011 - Proceedings 2011 International Conference on Business Management and Electronic Information, 2:483–487. <https://doi.org/10.1109/ICBMEI.2011.5917952>
- Zhang L, Einstein H (2004) Using RQD to estimate the deformation modulus of rock masses. *Int J Rock Mech Min Sci* 41:337–341. [https://doi.org/10.1016/S1365-1609\(03\)00100-X](https://doi.org/10.1016/S1365-1609(03)00100-X)
- Zhou J, Dai Y, Khandelwal M, Monjezi M, Yu Z, Qiu Y (2021) Performance of hybrid SCA-RF and HHO-RF models for predicting backbreak in open-pit mine blasting operations. *Nat Resour Res* 30(6):4753–4771
- Zhu W, Nikafshan Rad H, Hasanipanah M (2021) A chaos recurrent ANFIS optimized by PSO to predict ground vibration generated in rock blasting. *Appl Soft Comput* 108

Publisher's note Springer Nature remains neutral with regard to jurisdictional claims in published maps and institutional affiliations.